

**Extracellular Recording of Retinal Neurons Using Novel Multi-electrode  
Microarray System**

A Thesis Submitted in Partial Satisfaction  
Of the Requirements for the Degree of  
Bachelor of Science in Applied Physics  
at the  
University of California, Santa Cruz

By

Sabra I. Djomehri

March 19, 2009

-----  
Alexander Sher  
Technical Advisor

-----  
David P. Belanger  
Supervisor of Senior Theses,  
Chair, Department of Physics

**Abstract**

The retina, which lines the inner surface of the eye, receives information from the visual world and then processes and transmits it to the central nervous system. Cells called neurons make up this retinal tissue, and send long wire-like projections to the brain to transport processed information in the form of electrical signals called action potentials, or spikes. These cells, however, do not act independently; it is now thought that neurons function with other neurons in a group. To study this, an extracellular recording method utilizing a 512 electrode microarray system was developed. Extracellular techniques involve placing electrodes near neurons and recording changes in membrane potential, indicating the presence of a spike. Single electrode extracellular recording has been done extensively in previous years, which can only measure the output activity of a single neuron. However, a multi-electrode extracellular approach can record activity from many neurons. In the Santa Cruz Institute of Particle Physics, a microarray consisting of 512 electrodes in rectangular geometry was fabricated, with electrodes spaced at 60  $\mu\text{m}$ . These specifications are purposely congruous with that in the neuronal system of the retina; the spacing of neurons must match the spacing of electrodes in order to accurately identify neuronal patterns of spike activity. Also, neurons must fully occupy a local area to match the density of electrodes on the array system. Before performing retinal experiments with these arrays, the arrays themselves need to be tested. There were in total 99 arrays, and each was tested for the presence of shorts between pairs of electrodes. The threshold resistance between channels is  $\sim 10^7 \Omega$ , any resistance found below this point was considered a short. The testing determined that approximately 25% of arrays contained zero shorts.

## **I. Introduction**

The nervous system consists of a network of specialized cells called neurons and glia. Neurons are the main signaling unit of the nervous system, while glia are supporting cells that aid in the function of neurons. Neuronal cells communicate with each other through the transmission of electrical impulses called action potentials, or “spikes” [1]. These spikes propagate along an axon, the part of the neuron which carries signals and relays them to other neurons through the process of synaptic transmission.

The human brain contains as many as one hundred billion ( $10^{11}$ ) neurons [9]. It is now thought that information about the external world is processed by the activity of neuronal clusters rather than by single neurons. Extracellular recording is a technique that measures action potentials by placing an electrode near a neuron and detecting changes in membrane potential. Single electrode recording can only record information from one neuron, whereas multi-electrode experiments involve a large number of electrodes capable of acquiring spike information from tens to hundreds of neurons. In this method, membrane potentials from hundreds of neurons are simultaneously recorded at hundreds of spatial locations, which allows for detecting patterns of activity within a neuronal cluster. Understanding how neurons interact with one another may reveal important discoveries about brain function and how we interpret the world.

At the Santa Cruz Institute of Particle Physics (SCIPP), a microarray with 512 electrodes was fabricated. The diameter of each electrode is  $5\ \mu\text{m}$ , and the distance between electrodes is  $60\ \mu\text{m}$  [6]. The requirements of such an advanced system must parallel the scale of a given neuronal system, in this case, the retina. For example, the spacing of retinal neurons should be analogous to the spacing between electrodes, and the number of neurons in a cluster should correlate to the number of electrodes. A recorded signal from an array can be readout by a circuit board called the Neuroboard,

amplified by Neurochips, and recorded through the data acquisition program Labview [4]. Information is recorded at a rate of 15 MB/s onto a hard disk. The sampling rate for this system is 20 kHz/channel at a 12 bit resolution [4]. Multiple neurons can be detected by an electrode, and also different electrodes can pick up the same neuronal cell. This information is represented by the analog signals of various electrodes, which show different spike amplitudes for each cell.

The retina itself is composed of three basic layers— the photoreceptors (which receive input signals in the form of light), the intermediate cells (horizontal, bipolar, amacrine), and the retinal ganglion cells (RGCs) which encode light received into electrical signals that are relayed to the brain via the optical nerve [9]. In the mammalian retina, there have been roughly two dozen different types of RGCs found. In retinal experiments conducted at SCIPP, retinal tissue is manipulated by placing the RGC layer face down on top of the microelectrode array where it is then allowed to respond to a visual movie shown to it. This is a special movie made for the purpose of the experiment, showing a grid with alternating black and white (or even colored) squares. What is shown in a movie is always known, which gives the experimenter control over the exact input of light is delivered to the retina. This way, the electrical output of hundreds of RGCs can be measured and analyzed.

## **II. Background Information**

### ***The Action Potential***

Nerve cells (neurons) communicate to one another by producing an electrical signal called an action potential. The action potential itself is an electrochemical impulse generated when positive ions flow in and then out

through channels on a neuronal membrane. A spike can initiate another to occur next to it, which subsequently induces another, and so on across the entire length of the axon; this acts like a self-regenerating wave [9]. These signals are transmitted long distances across the axon, and are received by the dendrites (input receiving structures) of a post-synaptic neuronal cell through the events of synaptic transmission. The end result is the generation of a potential in a receiving neuron that alters its excitability. Despite being poor conductors of electricity, neurons have evolved complex ways of generating action potentials due to ion fluxes across their plasma membranes. Three main requirements for the quick and efficient generation of an action potential are: 1) voltage-dependent mechanisms, 2) membrane depolarizability towards threshold, and 3) propagation along myelinated axons.

Cells in the body maintain a low concentration of sodium and a high concentration of potassium. This is accomplished through the active transport mechanism, which utilizes a  $\text{Na}^+/\text{K}^+$  pump that moves sodium and potassium ions against their concentration gradients. In order to move these ions against their gradients, energy is needed in the form of ATP, or activation by the molecule adenosine triphosphate [1]. This pumping of ions results in more positive charges leaving the cell than coming in, which generates a buildup of positive charge outside the cell compared to inside it. This difference in charge between the outer and inner membrane allows spikes to be initiated in a nerve cell. Each pump binds three sodium ions and transports them out of the cell, then binds two potassium ions and carries them inside. In a neuronal cell, the resting potential is negative, usually between -40 to -90 mV. [9]. When an action potential is produced, the membrane potential becomes transiently positive (to around +20 to +40 mV), indicating a brief rise in  $\text{Na}^+$  permeability [9]. The cell machinery that

allows for depolarization are voltage-gated Na<sup>+</sup> and K<sup>+</sup> channels. When these channels open, they allow Na<sup>+</sup> and K<sup>+</sup> to flow down their concentration gradients. Their ability to open or close is influenced by a change in membrane potential. While hyperpolarization keeps these gates closed, a depolarization in the membrane will be detected by voltage sensors, allowing gates to open. At rest, the inside of a cell is negative while the outside is positive. At the instant the gates open, the inner environment of the cell is still negative, which physically attracts Na<sup>+</sup> ions to flow in. This sudden increase in sodium ions makes the inside more positive; this creates a repulsion effect with the potassium ions inside the cell, causing them to flow out. Shortly after, the sodium channels become inactivated, while potassium ions are still leaving the cell. This efflux causes the inner cell to become less and less positive (hyperpolarization) in an attempt to return the membrane to its resting potential.

Action potentials have a threshold that controls their fate. If one has been initiated at a particular membrane potential, then it has successfully crossed a threshold. All action potentials need some depolarizing stimulus that brings the membrane to this threshold level. The electrical potential generated across the membrane at electrochemical equilibrium is known as the equilibrium potential, and can be found using the Nerst equation,

$$E = \frac{RT}{zF} \ln \frac{[\text{ion outside cell}]}{[\text{ion inside cell}]}$$
, where R is the universal gas constant (R= 8.314 J K<sup>-1</sup> mol<sup>-1</sup>), T is the absolute temperature, z is the ion charge, and F is the Faraday constant (F = 9.65 x 10<sup>4</sup> C mol<sup>-1</sup>) [9]. The brackets indicate the ion concentration outside the cell divided by the ion concentration inside the cell. The equilibrium potential of a cell is the potential at which there is a balance between the concentration gradient and the electrochemical gradient; there is no net flow of ions. This potential lies between -100mV and

+70mV [9]. When the cell depolarizes, the potential is driven towards the reverse potential. When  $E$  is above the threshold, the probability of an action potential occurring increases (excitatory); when  $E$  is below threshold, the probability for a spike to occur decreases (inhibitory). When signals are communicated between neurons at regions known as synapses, there is a release of neurotransmitters. Neurotransmitters are molecules that bind to the receptors on a receiving (postsynaptic) neuron, causing them to either open or close. Activation of these receptors (called ligand-gated channels) allows ions to flow across the postsynaptic membrane, which causes a depolarizing current to be generated in the axon hillock [3]. This depolarization generates a change in membrane potential at this site, which generates another spike. Figure 1 shows an excitatory synaptic event that led to the creation of an action potential by a disturbance in membrane potential.

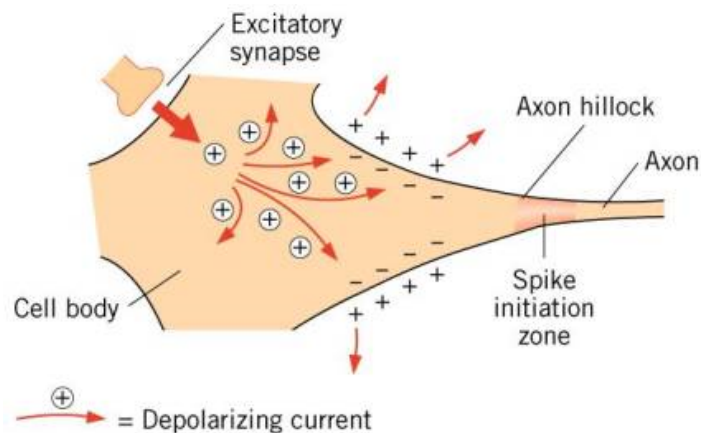


*Figure 1. Site of spike generation. [3]*

The resulting neurotransmitter-induced current flow changes the membrane potential of the postsynaptic neuron, increasing or decreasing the probability that it will fire an action potential. A single neuron can receive as little as one to more than a thousand synapses depending on its function and where it's found in the nervous system; in other words, there are many types

of neurons that can receive largely varying numbers of synapses [9]. Some of these synapses are excitatory while others are inhibitory. The sum of all these events determines whether or not an action potential is fired; if the sum of all synaptic events is above threshold, then an action potential will occur.

The key voltage-dependent events that generate action potentials occur in the following order in a cell, one after another: activation of sodium ion conductance, activation of potassium ion conductance, and inactivation of the sodium ion conductance [9]. Figure 2 below shows these events by representing sodium conductance ( $g_{Na}$ ) in purple and potassium conductance ( $g_K$ ) in green. The dotted curve shown is the superimposition of both purple and green curves, representing the actual action potential generated. When the membrane depolarizes,  $Na^+$  channels open allowing an influx of sodium ions into the cell, called the depolarizing (rising) phase. This increase of  $Na^+$  current further depolarizes the cell towards a maximum value (the overshoot), followed by a sudden inactivation of  $Na^+$  conductance. As  $Na^+$  current decreases,  $K^+$  conductance has been steadily on the rise; this contributes to the falling phase of the action potential. Since depolarization doesn't inactivate potassium channels, these ions proceed to hyperpolarize the membrane, known as the undershoot [3].

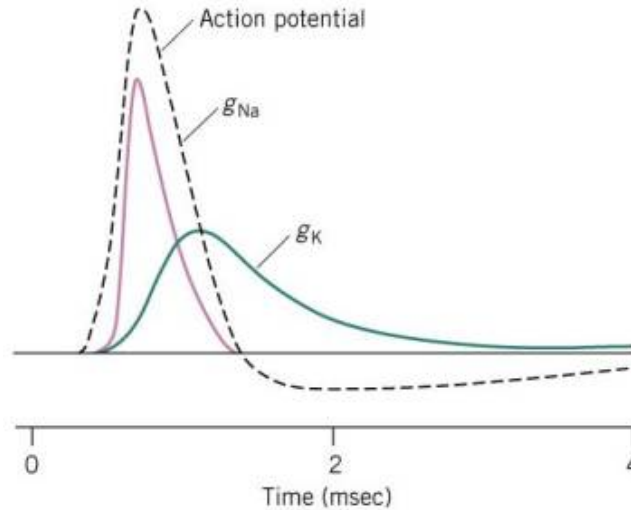


*Figure 2. Superimposition of sodium/potassium conductance curves. [3]*

At this point, the membrane is temporarily more negative than its resting potential. This is short lived since the hyperpolarization itself causes  $K^+$  conductance to inactivate, returning the membrane potential back to its resting potential. Sodium activation and inactivation occur quickly, relating to the sharp peak of the purple curve in Figure 2, whereas the potassium activation occurs slowly and steadily decreases.

In addition, there is a short amount of time, called the refractory period following an action potential in which the cell is resistant to more excitation. It occurs when the membrane is hyperpolarized due to an efflux of  $K^+$  ions. During this interval, about 2-3 ms, a second action potential can't be initiated no matter how large the stimulus is because  $Na^+$  channels have been inactivated [8]. These channels will remain inactivated until the membrane returns to its resting potential and they regain their ability to open in response to a stimulus. Also, action potentials exhibit all-or-none behavior, which means only if a stimulus is larger than a certain threshold in the cell will a spike be generated; any amount lower than this threshold, no

spike will arise. The refractory period is important in allowing the action potential to regenerate itself continually along the axon. The action potential itself makes it momentarily impossible for the axon to generate more; this limits the amount of spikes that a neuron can produce per unit time. This refractory period occurs in the membrane region where the spike was initially generated, and such resistance to subsequent excitation prevents action potentials from propagating backward. This behavior ensures the forward propagation of action potentials from the point of initiation to the synaptic terminals. Also, it is important to note that action potentials within a cell always have the same amplitude; however it is the frequency of spikes occurring that indicate the strength of a signal and carries information to encode the signal.

The conduction rate of an action potential presents a limiting factor for the flow of electrical signals (information) in the nervous system. Action potentials move along unmyelinated axons at speeds of maximum 10 m/s [8]. However this is too slow for normal function, and has been accounted for by the adaptation of the myelin sheath surrounding axons, shown in Figure 3.

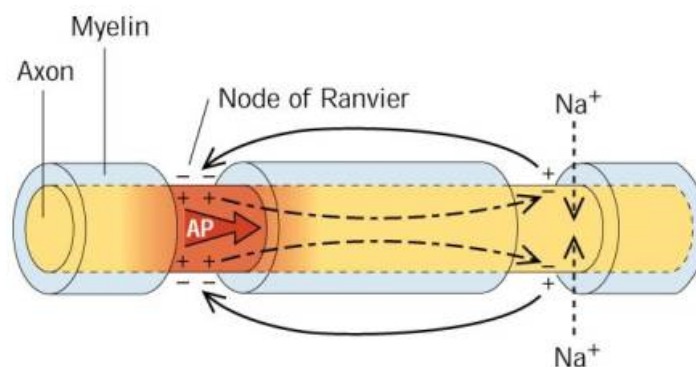


*Figure 3. Action potential propagation through axon with myelin sheath. [3]*

With these, spikes can reach speeds of up to 120 m/s [8]. The myelin sheath insulating the axons decreases the internal resistance to passive current flow by increasing the diameter of the axon. This results in an increase in action potential conduction velocity. Also, the myelin sheath prevents possible current leakage out of the axon, and in this way also increases the distance along which the electrical signal can travel. The Nodes of Ranvier, shown in Figure 3, are places along the axon where gaps are present between myelin sheaths [3]. However, since these nodes are the only sites where the axon is not insulated by the sheath, they allow electrical impulses to be generated. Thus, they are very important in spike production since ion channels can exist there in order for depolarization to occur. The sheath that covers the axon closes sodium channels (except at the nodes), resulting in an action potential that jumps from node to node and relates to the very fast velocities a signal can travel [8].

For an action potential to proceed, it requires both active and passive current flow. As  $\text{Na}^+$  channels open, some of the depolarizing current flows passively down an axon, which causes a local depolarization in neighboring  $\text{Na}^+$  channels. This opens them, and generates a subsequent action potential in the adjacent region to the initial site of activation. During this period, the initial  $\text{Na}^+$  channels inactivate, potassium flows out, and the membrane potential repolarizes and marks the axon as refractory in that region. Meanwhile, the new action potential that occurred similarly creates a local depolarization downstream in the axon, and another action potential is generated. This pattern is a chain reaction of depolarizing events which are

together responsible for carrying the spike across the entire length of the axon.

### ***Retina***

The retina is the innermost layer of the eye which contains neurons that receive, process, and send information acquired from the outside world to the brain in the form of electrical signals. Even though the retina is located peripherally to the brain, it's still part of the central nervous system. It displays complex neural circuitry that transforms the graded electrical activity of specialized light sensitive nerve cells, called photoreceptors, into spikes leading to the brain via the optic nerve. There are five classes of neurons which exist in the retinal layer: photoreceptors, bipolar cells, horizontal cells, amacrine cells, and ganglion cells, shown in Figure 4 [9].

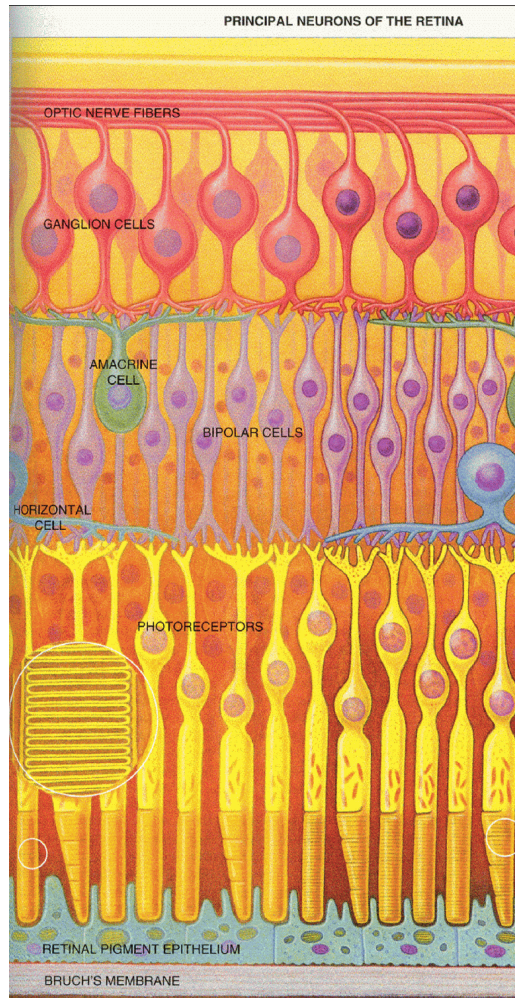


*Figure 4. Structure of the retina. [9]*

The photoreceptor layer consists of cells called rods and cones, which are distinguished by shape and distribution across the retina. The rod system (rod shaped photoreceptors), has very low spatial resolution but high sensitivity to light, meaning that its functionality specializes in sensitivity to light at the expense of resolution. On the other hand, the cone system (cone shaped photoreceptors) has very high spatial resolution while being relatively insensitive to light, meaning that its functionality is specialized for visual acuity at the expense of sensitivity [9]. In the day time, rods are inactive due to being saturated by light, and so are used only in the night time when light levels have decreased. Cones dominate during the day since

they aren't as sensitive to light as rods are, and account for our day vision. However, rod density far exceeds cone density, with 90 million rods to 4.5 million cones in the retina [9]. Despite this imbalance, cones compensate by increasing in density 200-fold in the fovea, a highly specialized region that mediates high levels of visual acuity [9].

The synaptic terminals of photoreceptors contact the bipolar and horizontal cells. The basic three neuron circuitry of the retina is photoreceptor to bipolar cell to ganglion cell; this pathway transmits visual information to the brain. Horizontal cells facilitate lateral interactions between photoreceptors and bipolar cells that are involved in maintaining visual sensitivity to contrast. Amacrine cells play important roles in the pathway from rods to ganglion cells and are important for the selective directional responses manifested by certain types of ganglion cells [9]. These cells can support or inhibit pathways between bipolar and ganglion cells, where they are presynaptic to ganglion cells and postsynaptic to bipolar cells. Also, they provide additional connections between bipolar and ganglion cells.

In the retina, only ganglion cells generate action potentials (and some amacrine cells), while all other cells use graded potentials due to their small sizes [1]. For example, when light is absorbed by the photoreceptors, this generates a small graded change in membrane potential and neurotransmitters are released onto postsynaptic bipolar cells, which also generate graded potentials. Since photoreceptors and bipolar cells are so small, transmitted information passes fairly short distances. Due to this, spikes can't actually be initiated, but instead, a small graded potential occurs that causes a depolarization in adjacent cells in the pathway. When this depolarizing stimulus reaches a ganglion cell, an action potential is generated along the optic nerve and goes all the way to the brain, where

information is received in the form of electrical signals. Ganglion cells are able to produce spikes due to their axons being much larger than all other classes of retinal cells. The general pathway for light to be received, processed, and sent to the brain is: photoreceptor→bipolar cell→ganglion cell→brain.

### **III. Methods of Detecting Electrical Activity of Neurons**

#### ***Extracellular vs. Intracellular Recording***

There are two major ways to measure neural activity— by extracellular recording and intracellular recording. In extracellular recording, microelectrodes are placed near neurons, and action potentials are measured. The actual measurement is the voltage difference between two different points, one near the membrane and another being a reference point. In the central nervous system of mammals, a recorded spike lasts only 0.5-1 ms, and has amplitudes in the range of a few hundred microvolts [1]. However, the spike accounts only part of the action potential; the hyperpolarization following the spike can last as long as 5-15 ms, and the subsequent return to resting membrane potential can last between 50-80 ms [1]. In addition, there exists a given noise amplitude which is produced from the microelectrodes themselves, usually in the range of a few microvolts. The method of extracellular spike detection using a multi-electrode system is useful for detecting patterns of neural activity, and is quite advantageous due to its “in vitro” (i.e. taking place in a living laboratory) approach; neurons can be recorded without damaging them through puncturing electrodes into the cell. Figure 5 below shows an example of the extracellular recording of a single neuron [7].

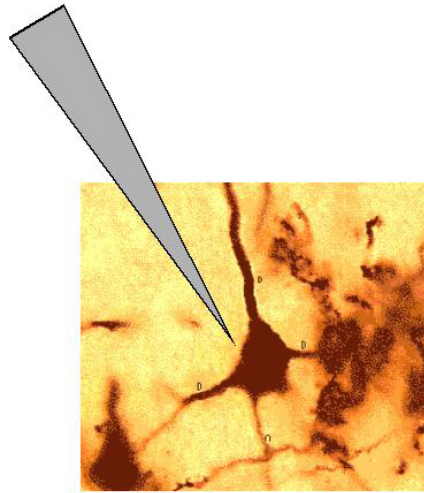


*Figure 5. Extracellular recording of a single neuron. [7]*

Living retinal tissue is extracted from a mouse, placed on top of an array, and immersed in saline solution to keep it alive for roughly 15 hours (much longer than the average duration of one experiment). Each neuron leaves behind a special “footprint” of activity in the form of spikes. In a multi-electrode system, these various “footprints” or patterns created by each different neuron can be distinguished apart; this is impossible using a single electrode system. For example, when only one electrode is present, spikes from two different neurons can be picked up but it would be impossible to tell which neuron each spike came from. However, if there are two electrodes present in a local area, a neuronal signal will be picked up by the closest electrode and not by the one farther away. If a neuron is between both electrodes, it will be picked up by both electrodes. In this way, neurons can be distinguished from one another based on which electrode picks up its signals, and the specific shape formed by a signal. When it is known which neurons generate which signals, neurons can be classified due to the special signal patterns they generate.

Intracellular recording is a method of spike detection in which an electrode is placed inside a neuron and the voltage across the membrane is measured. The intracellular recording experiments performed by Hodgkin and Huxley in 1963 provided the foundation to understanding how action potentials are produced [9]. The basic technique consists of placing a glass pipette inside a cell, which has a tip diameter of less than 1  $\mu\text{m}$  and resistance in the megaohm range [9]. In the extracellular approach, only action potentials can be detected but in intracellular recording, both action potentials and smaller graded potential changes can be picked up. For example, if a single input generated only a graded potential and no spike was produced, the intracellular electrode will be able to detect it. These smaller potential changes are signals that failed to produce action potentials due to being lower than threshold. A major advantage of this method is its ability to directly measure the electrical activity of a single neuron by inserting a microelectrode inside the cell. Despite this gain, the life span of the cell is drastically decreased. In order to maximize efficiency using this technique, the size of the electrode's tip should be minimized as much as possible to ensure minimal cell damage. However, as the size of the tip decreases, the electrical resistance increases. Although a very small tip may generate very low damage to the cell, its resistance may be so large that changes to membrane voltage (i.e. spikes) become unidentifiable in between the large thermal noise.

### ***Patch Clamp Technique***

Modern intracellular experiments use a fine tip glass pipette containing a tiny opening. This opening is used to make contact to a small patch on the neuronal membrane. Suction is applied to the membrane, producing a very tight seal between it and the pipette such that there can be no flow of ions. This method is called a cell-attached patch clamp, and there is only one

channel within the pipette. In the event that a single channel opens, then ions will flow into the pipette. The patch clamp setup is shown in Figure 6 [9].

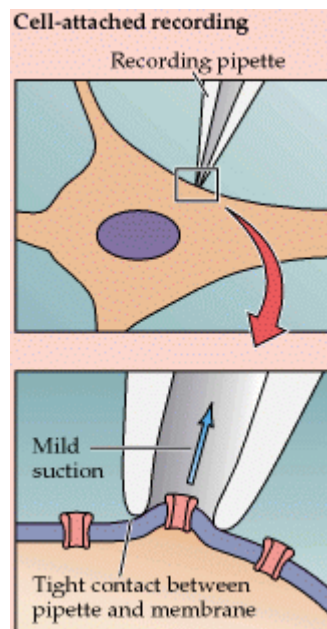


*Figure 6. Patch Clamp Technique.[9]*

Even though the amount of ions flowing into the pipette is very small, the current can still be detected using an amplifier which is connected to the pipette. In whole-cell recording, there is a strong pulse of suction applied to the membrane patch, and the cytoplasm of the neuronal cell becomes continuous with the inside of the pipette. Using this technique, one can measure the currents and potentials from the whole cell. In another technique known as inside-out recording, a small portion of the membrane is detached from the cell by the pipette. This exposes the intracellular surface of the cell, and the pipette is similarly exposed to the air. In this configuration, the currents of single channels can be recorded. This recording is done due to the membrane patch being attached to the pipette, which creates a continuous surface from the intracellular membrane surface to the inner pipette surface. This method is particularly useful in

understanding how the behavior of intracellular molecules affects the functionality of ion channels. Patch clamp experiments have shown the properties of ion channels that influence potassium currents in action potentials.

### ***Voltage Clamp Technique***

The Na<sup>+</sup> permeability that generates a change in membrane potential is itself sensitive to the membrane potential, which creates difficulties when studying the mechanism behind action potentials. This difficulty lies with varying the membrane potential to analyze changes in permeability; when changes in membrane potential occur, this causes more uncontrolled changes. Using the voltage clamp technique, one is able to control membrane potential while measuring the changes in permeability. This is done by a microelectrode placed inside a cell that controls or “clamps” a voltage at any level. An internal electrode measures  $V_m$ , the membrane potential, and is connected to the voltage clamp amplifier [2]. This amplifier compares  $V_m$  to the holding potential, or “command voltage”, which an experimenter has set to be the “desired voltage” that is to be maintained in the cell. When  $V_m$  is different than the command potential, the clamp circuitry uses a negative feedback to pass a current back into the cell through a second electrode, which is outside the cell. This second electrode is used as a reference electrode. The internal electrode maintains a constant voltage at a desired level by sending a current into the cell. The current that is measured is equal to the current needed to keep the cell membrane at the desired potential. This technique reveals how membrane potential influences ionic current flow across a membrane. It was developed by Kenneth Cole in the 1940s and was first done on membrane currents in squid

giant axons [9]. Figure 7 shows the circuitry for this feedback arrangement [2].

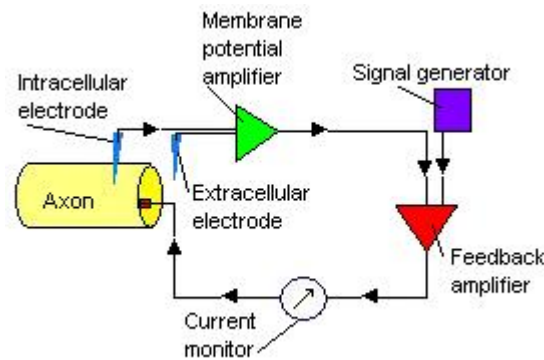


Figure 7. Circuitry for the voltage clamp technique. [2]

### **Current Clamp Technique**

Using the current clamp technique, a current is injected into a neuron by an electrode which records the membrane potential. In this case, the cell membrane is not held at a fixed voltage but rather, is allowed to vary. An amplifier then records the voltage that is generated by the cell either of its own accord or by a given stimulation. The main significance of the amplifier is not to provide amplification, but instead to preserve the accuracy of measurements by slightly changing small signals produced by cells. The device is called an electrometer, which is able to increase the current while decreasing the resistance as the current passes. In effect, the electrometer transforms a high impedance signal to a low impedance signal. This is called a “unity gain” buffer amplifier, which has the following circuit diagram shown in Figure 8 [5].

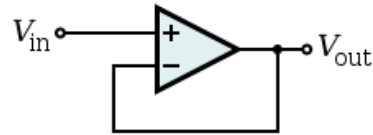


Figure 8. Circuitry for the unity gain buffer amplifier in current clamp technique. [5]

The output of the amplifier is connected to its input in a negative feedback arrangement, which translates into output voltage equaling input voltage. By utilizing this technique, experimenters are interested in understanding what happens to a cell when current is transmitted through it. This reveals an important consequence for neurons. When a current is injected across the membrane, an action potential may be generated. As ion channels open, this causes changes in membrane potential and conductance, which lead to sodium and potassium fluxes. This mechanism is important in understanding how neurons react to certain neurotransmitters, which can either activate or deactivate ion channels in the membrane.

### **Single Electrode vs. Multielectrode Recording**

In the field, many techniques are used to model neural systems. These range from models of the short-term behavior of single neurons to models aimed at understanding the complex interactions between a group neurons. In the past, single unit recording provided a way to quantitatively analyze patterns of electrical signals recorded from individual neurons. In this extracellular technique, a single electrode is used to measure spikes generated from one neuron. The tip of a microelectrode is usually about 1 micron in diameter, and is introduced in living brain tissue. The spike activity from a nearby neuron produces signals of about 0.1 mV [9]. Despite providing important information regarding brain function, this method is only capable of determining the behavior of individual neurons. However, in

understanding how the brain processes information it is necessary to consider the interactions and behaviors of neural networks. This is done using a multi-electrode technique that can detect patterns of electrical activity from tens to hundreds of neurons at a time. An arrangement of microelectrodes is fabricated and live brain tissue is placed on top of it, where each electrode picks up spike signals from an adjacent neuron. In order for this to be successful, the spacing between neurons must match the spacing between each electrode. The neural spacing of brain tissue is on the order of microns.

### ***512 Electrode Arrays***

At the Santa Cruz Institute of Particle Physics (SCIPP), researchers have developed a detector which utilizes a 512-electrode system to identify spikes from hundreds of neurons. The 512 electrodes are spaced at 60  $\mu\text{m}$  apart and are in a rectangular shape [4]. However, the geometry preferred by experimenters is actually a hexagonal shape; this allows traces (wires) connected to the electrodes to have more flexibility in branching away from one another (to avoid crowding). In this case, the rectangular layout is used due to the spacing of electrodes and line widths of 4  $\mu\text{m}$ . Figure 9 shows three different array geometries that have been used by neuroscientists; the conventional single electrode system that records a single neuron, a 61 electrode system spanning a hexagonal area, and the new 512 electrode system being described here [4]. The circular area represents the visual sensitivity area of a neuron in the part of the visual cortex that detects motion.

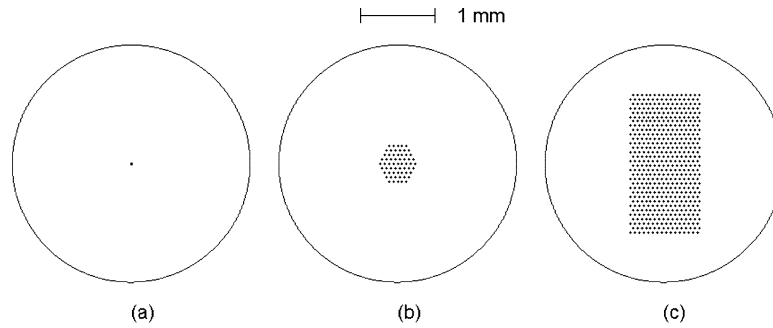


*Figure 9. Electrode array geometries of a) single electrode, b) 61 electrodes and c) 512 electrodes. [4]*

Photolithography and wet etching techniques were used in the fabrication of these arrays. Figure 10 shows the 512 electrode array with 128 bond pads on each of the four edges [6]. The bond pads have a pitch of 200  $\mu\text{m}$  and readout to the Neuroboard (Figure 11) [4]. In determining the patterning of the array, a 150 nm layer of the conductor indium tin oxide (ITO) is applied to a glass substrate [6].

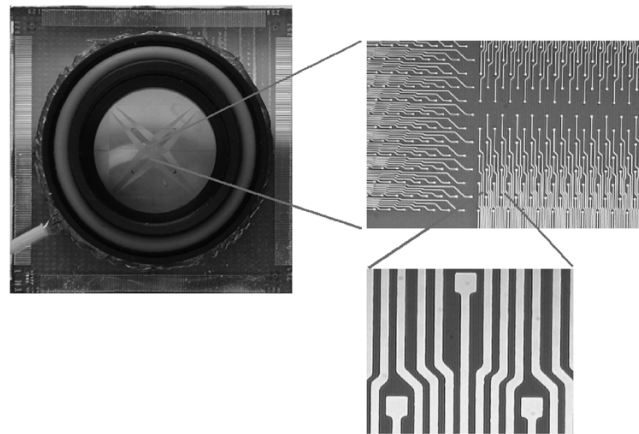


*Figure 10. 512 electrode array with schematic of ITO wires. [4]*

Following this, a layer of Molybdenum (Mo) is placed over the ITO layer, along with a 1  $\mu\text{m}$  photoresist layer (Shipley-3612-resist) [6]. The photomask is used to expose these three layers (ITO, Mo, photoresist) to the pattern created by the UV light. The photoresist is left on top of the places where the desired traces are meant to be, and the rest will be exposed to UV light.

Then, a plasma etching is used to remove the exposed Mo, followed by a liquid etching used to remove exposed ITO. Next, the photoresist is dissolved and the remaining Mo is taken away by plasma etching. After these steps are complete, the ITO traces will only be left on the glass.

The exposed ITO wires are then insulated and buried by a 2  $\mu\text{m}$  layer of silicon nitride, which has a high strength over a wide temperature range [6]. This “passivation” layer is also necessary for the connection of ITO wires with the bond pads, which are themselves covered by a 1  $\mu\text{m}$  layer of aluminum to enable good electrical contact with wire-bonding and probes. The 512 array has an impedance of 200  $\text{k}\Omega$  at 1 kHz, while ITO traces have impedances of 5  $\text{k}\Omega$  [4].

After fabrication, the array is connected to a circuit called the “Neuroboard” shown in Figure 11 below, with the 512 array glued to the center. The array reads out to 8 Platchips and 8 Neurochips which utilize ac-coupling. The Platchips provide AC coupling, while the Neurochips amplify and multiplex the signals [4]. The chamber in the center defines a boundary for the system containing the electrodes, retinal tissue, and saline solution keeping it alive for roughly 15 hours during an experiment. When the array is filled by the saline solution, the input noise is about 7  $\mu\text{V}$ , and the threshold signal amplitude is 60  $\mu\text{V}$  [4]. A typical experiment will acquire 0.3 terabytes of data. Analysis of the data reveals that an electrode can measure signals coming from different neuronal cells, and also that a neuron can be recorded on many different electrodes.

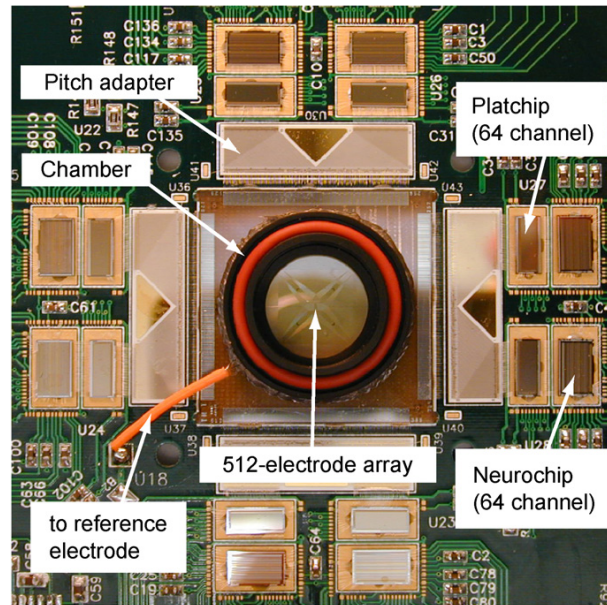


*Figure 11. Neuroboard with 512 electrode array connected in the center. [4]*

Not all of the 512 electrode arrays were made with exactly the same features. So far, two batches of arrays have been fabricated, where four arrays are made together on a given wafer. In the first batch, two arrays were made as described above, but the other two contain an extra layer of Molybdenum that was purposefully not plasma etched along with the resist layer. The presence of Molybdenum (Mo) on the array can be seen visually as a shaded pattern. The particles of this layer not only exist on top of the ITO wires, but also in between the wires. This increases the conductivity between wires due to the conductive properties of Molybdenum. In the second batch, the first three arrays on the wafer have electrodes spaced at 60  $\mu\text{m}$  apart, whereas the fourth array contains electrodes spaced at 120  $\mu\text{m}$  apart. Due to the electrodes being more spread out, the rectangular electrode geometry is not employed; instead, electrodes span a hexagonal area in the center of the array. The purpose of using a larger spacing of electrodes is to acquire spike potentials coming from neurons that are spaced farther from each other. To

detect neurons that are more widely spaced, the array area itself needs to be larger to be able to accurately assess the functional properties of neurons. If the number of electrodes is increased, this will increase the array's area but will create other difficulties in the readout system; more channels would have to be introduced. Instead, the number of electrodes is kept the same, but the distance between electrodes is increased. This method is used to detect retinal ganglion cells that are more widely spaced from each other. All these different neuron types can be classified based on a particular functionality within the retina.

### ***Impedance Measurements***

Before being used for experiments, the 512 electrode arrays are tested for damaged regions leading to shorts measurements between two electrodes. A short between two channels is a significant decrease in the impedance normally generated, and can be caused by a number of factors such as defective photoresist, dust particles, or some ITO not completely etched between traces. These factors arise due to errors in fabrication. The 512 array has an impedance of 200 k $\Omega$  at 1 kHz, and the impedance between adjacent channels on the multielectrode array is approximately on the order of 1 giga - 1 tera ohm [4]. The frequency, 1 kHz, matches the desired frequency for detected signals attained through the retinal experiment. Spike signals change over time, and AC coupling is used to block the DC component so that the AC component can be viewed with no visible DC offset. Shorted channels, defined on the order of 10 mega ohm and lower, display as sharp peaks on resistance graphs. Ideally, each pair of electrodes should have an infinite resistance between them. However since this can't be achieved, a parasitic resistance value,  $R_p$ , of larger than  $10^7 \Omega$  is accepted. When an array is used in a retinal experiment and immersed in saline solution, molecules of saline solution provide their own resistance values

between electrodes, called the “interface” resistance,  $R_i$ . In a pair of electrodes, each one has a resistance between it and a nearby conductive molecules, giving a combined resistance of  $2R_i = 4 \times 10^5 \Omega$  [6]. If the resistance between two electrodes is large, then its effect won't affect the array-saline solution system during the experiment. This is because the “circuit” of such a system is essentially a simple circuit with two resistors in parallel. The resistance then becomes:  $1/R = 1/R_p + 1/2R_i$ . If the value of  $R_p$  is near the same order as  $2R_i$ , this can affect the overall resistance since its value is no longer negligible. For example, if  $R_p = 10^5 \Omega$ , then the total resistance is going to be drastically lowered (nearly by a factor of two). Therefore, a necessary threshold has been approximated, indicating that any resistance measured below  $\sim 10^7 \Omega$  between a pair of electrodes is considered shorted. To note, the arrays with a Molybdenum layer will all contain  $R_p$  values that are somewhat lowered. This arises due to conductive Molybdenum particles between electrodes, which lowers the resistance between the channels to approximately  $\sim 10^8 - 10^9 \Omega$ .

### ***Instrumentation and Measurement Procedure***

The necessary equipment involved in determining impedances was a Cascade Microtech Probe Station, an array probecard, a Keithley 706 Scanner, a Keithley 237 High Voltage Source-Measure Unit, and a computer running the custom Labview code to control the equipment and store acquired data. The array probecard, which is stabilized just above the stage on the probe station, contacts the bond pads of the array and passes a constant voltage of 2V to the electrodes from the Keithley 237 voltage source unit. This generates a current that passes through the wires of the array circuitry and changes due to resistance between two channels. The source unit measures the current, and both the current and voltage are readout by the computer. The custom Labview program is able to

communicate between both the source unit and scanner, and controls the scanner in connecting consecutive pairs of electrodes to the source unit. Then, the code calculates resistance values based on Ohm's Law,  $V = IR$ , which can be rearranged to give the resistance as:  $R = V/I$ . The Keithley Scanner is responsible for switching between different pairs of electrodes. After reading one pair, it moves on to the next until all pairs of electrodes have been measured. However, since the probecard contains 33 probes, then only 32 pairs of channels can be measured at a given time. The probes are first positioned on the first set of 33 bond pads. After all 32 measurements are recorded there, the probes are physically lifted a distance above the array and shifted right in order to make contact with the next set of 33 electrode pads. This shifting of the probecard is done four times on each side of the array (128 electrodes per side), totaling sixteen times per array to account for all 512 electrodes. The last measurement on each side of the array is frivolous since it measures the resistance between the last channel and the glass substrate. The output resistances generated by the Keithley devices are plotted to a computer display using a custom Labview code. Resistance values are recorded on the y-axis and channel numbers are seen on the x-axis, going from 1 up to 32. The arrays themselves can be easily viewed either through the microscope on the Probe station, or by a program called Nucleus (containing a digital camera connected to a computer) that shows a widescreen representation of the array. Features on this program allow specific movements via joystick to portions of the array that will be contacted by the probes. The probecard's position is fixed firmly above the stage (where the array is placed), and the position of the array can be controlled by moving the stage in a 3-dimensional space. When the bond pads and probes are clearly visible and aligned together, a lever arm

on the probe station is pulled down to initiate contact of the probes on the array.

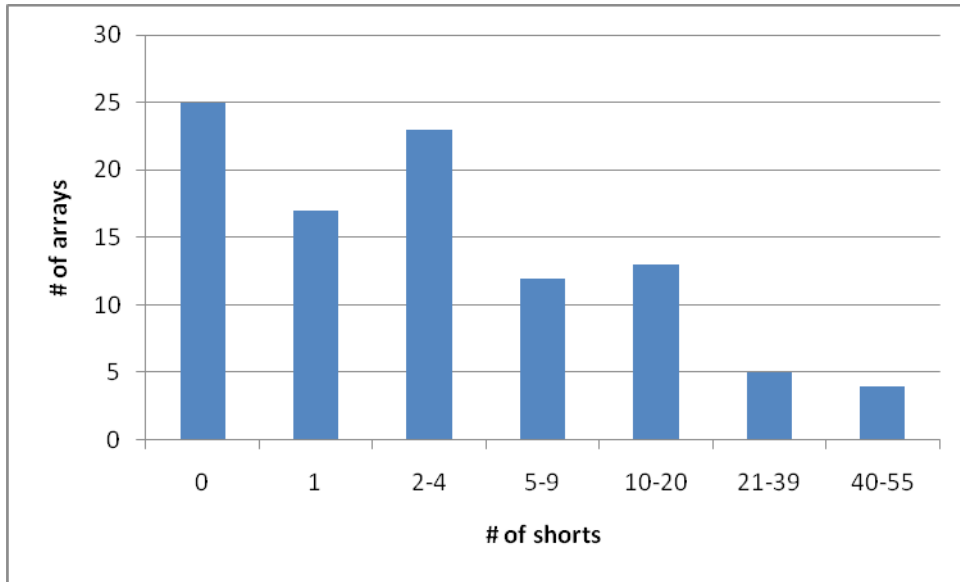
## IV. Results

Array testing measurements were acquired for a total of ninety-nine 512 electrode arrays. These arrays were named based on a systematic numbering system with three identification numbers written in sequence: 1) production batch number (1 or 2), 2) wafer number, and 3) array number on a given wafer. For example, if an array was produced in the second batch of arrays, on wafer number 4, and was the fourth array in the wafer (4 arrays per wafer), its systematic name would be: 2-04-4. In addition to an array's systematic name, it is also given an identification number (1-99) based on the chronological order the arrays were tested in. Of all the arrays, 23 were from the first batch containing the Mo arrays, while the rest were from the second batch containing both the 60 and 120 micron arrays. Table 1 shows the number of arrays having no shorts, 1 short, 2 to 4 shorts, etc. and provides the percentage of arrays having a specific number of shorts.

# of shorts	# of arrays	%
0	25	~25
1	17	~17
2-4	23	~23
5-9	12	~12
10-20	13	~13
21-39	5	~5
40-55	4	~4

*Table 1. Distribution of arrays by number of shorts.*

This data is also presented in the Graph 1:



Graph 1. Number of arrays vs. number of shorts.

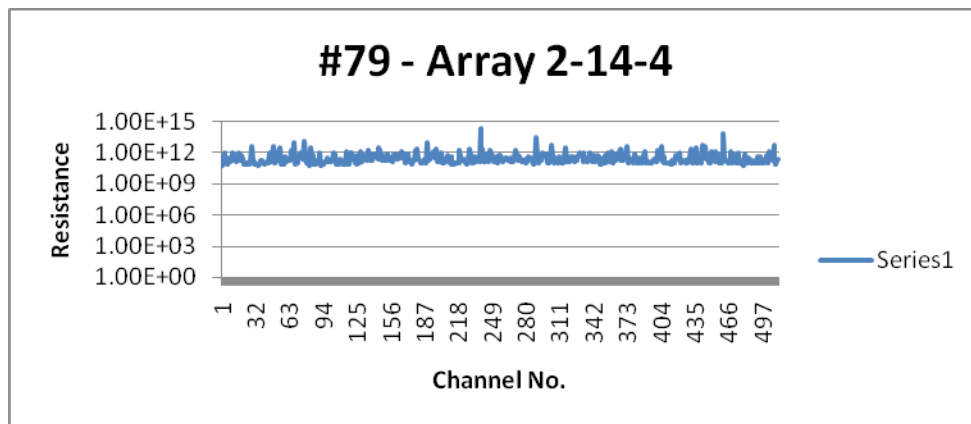
The largest percentage of arrays had no shorts at all, representing a quarter of all arrays. The next two largest groups of arrays had between 1-4 shorts, accounting for roughly 40% of arrays. Only four arrays had 40 shorts or greater, and less than 10% of arrays had greater than 20 shorted channels. Approximately 20-25% of arrays are in the middle range, having between 5-20 shorts. The 25 “perfect” arrays containing no shorts are listed in Table 2.

Array #	Array
3	2--01--3
9	2--07--1
10	2--07--2
11	2--07--3
14	2--09--2
16	2--09--4
20	2--12--4
36	1--2?--4
38	1--3?--2
39	1--3?--3
40	1--3?--4
41	1--4?--1
44	1--4?--4
54	2--02-3

69	2--08--2
75	2--10--4
77	2--14--2
79	2--14--4
85	2--18--2
89	2--22--2
91	2--22--4
92	2--23--1
93	2--23--2
95	2--23--4
97	2--24--2

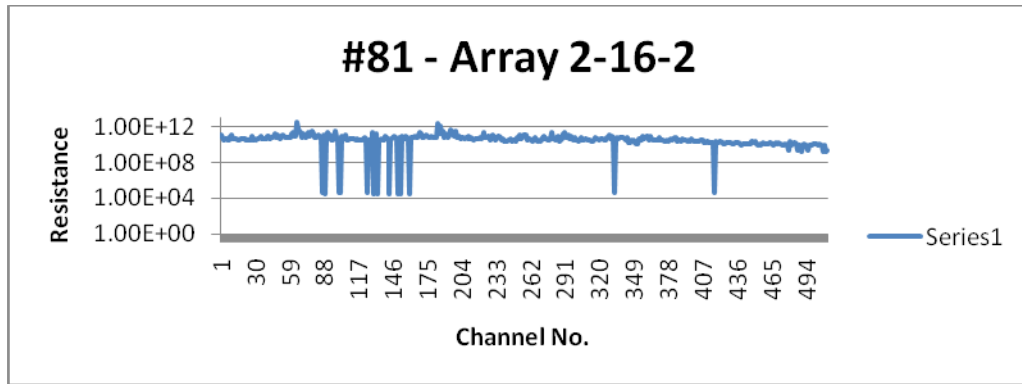
Table 2. Arrays with zero shorts.

The impedance measurements were saved as text files, where the raw data for each array was directly plotted based on a logarithmic scale. Impedance is shown on the vertical axis and the channel number is displayed on the horizontal axis. Graph 2 shows impedances values for array 2-14-4 (array #79), which is an example of a perfect array with no shorts. Typical resistance values are  $\sim 10^{11} \Omega$ .



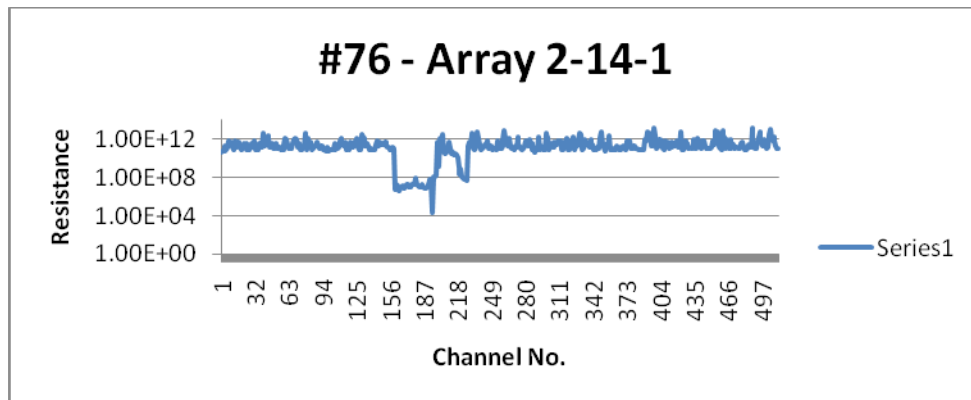
Graph 2. Impedance between adjacent channels as a function of channel number.

Another example is shown in Graph 3, this time displaying a “bad” array containing several shorted channels at various locations. Each peak represents a short occurring at  $\sim 10^4 - 10^5 \Omega$  and its location on the array can be identified by the channel number. Resistances found to be below the threshold of  $10^7$  ohms were considered as shorts.



Graph 3. Impedance vs. channel number for array #81.

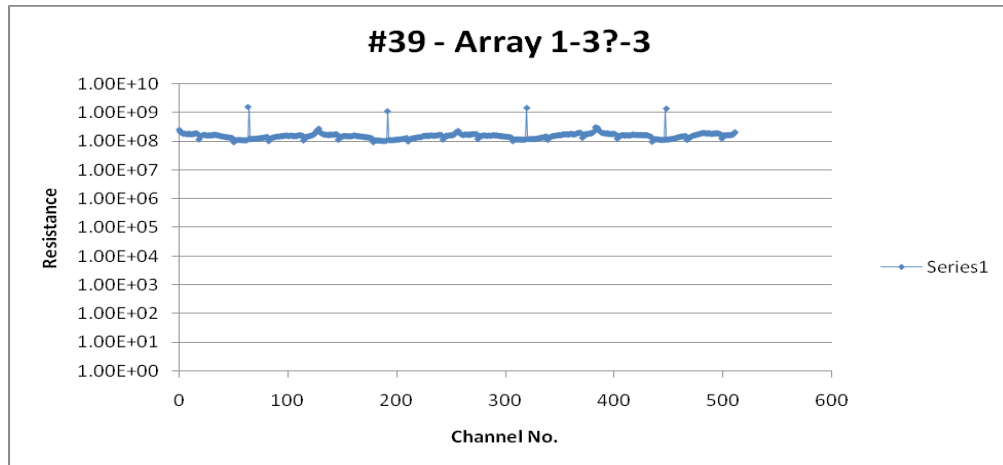
It is possible for an array to contain a patch of shorts, identifying an entire defective region on the array. Several channels are affected, indicating this wasn't simply a "fluke" event but a larger error that occurred during the fabrication procedure. Graph 4 shows impedance measurements for array 2-14-1, #76, containing a patch of shorts between channels 161-195.



Graph 4. Array #76 with a patch of shorts.

For arrays from batch 1 that contained a layer of Molybdenum over them, all resistances were determined, as predicted, to be consistently lower than arrays without this layer. Resistances were at  $\sim 10^8 - 10^9 \Omega$ . Also, there are four distinct peaks shown in Graph 5 that are higher than expected, and they each occur in the middle of all four sides of the array.

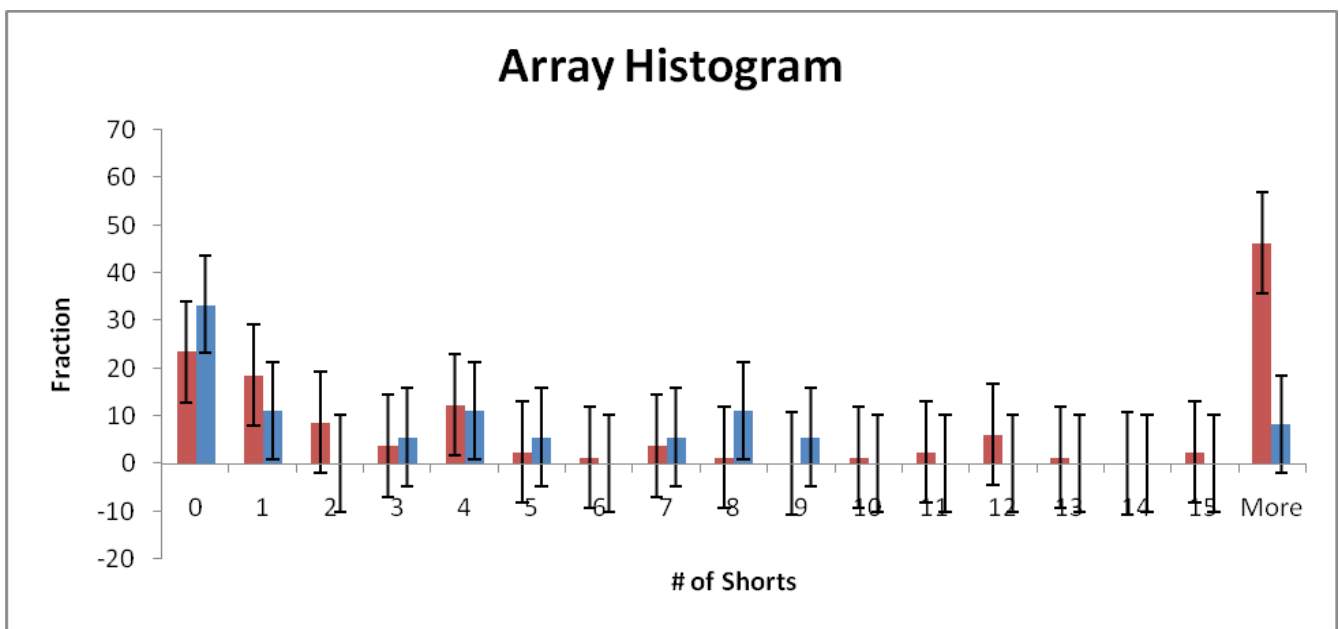
This is due to the way the ITO traces were arranged on the array; on each side, the traces run parallel to each other but then split in the middle to create an enlarged distance between those two split traces. Thus, when a resistance is measured between these channels, it will be much larger since the distance between the traces increased (due to being split apart). Graph 5 below shows array 1-3?-3 from batch 1 that contains a Mo layer.



*Graph 5. Array #39 with a Molebdynum layer.*

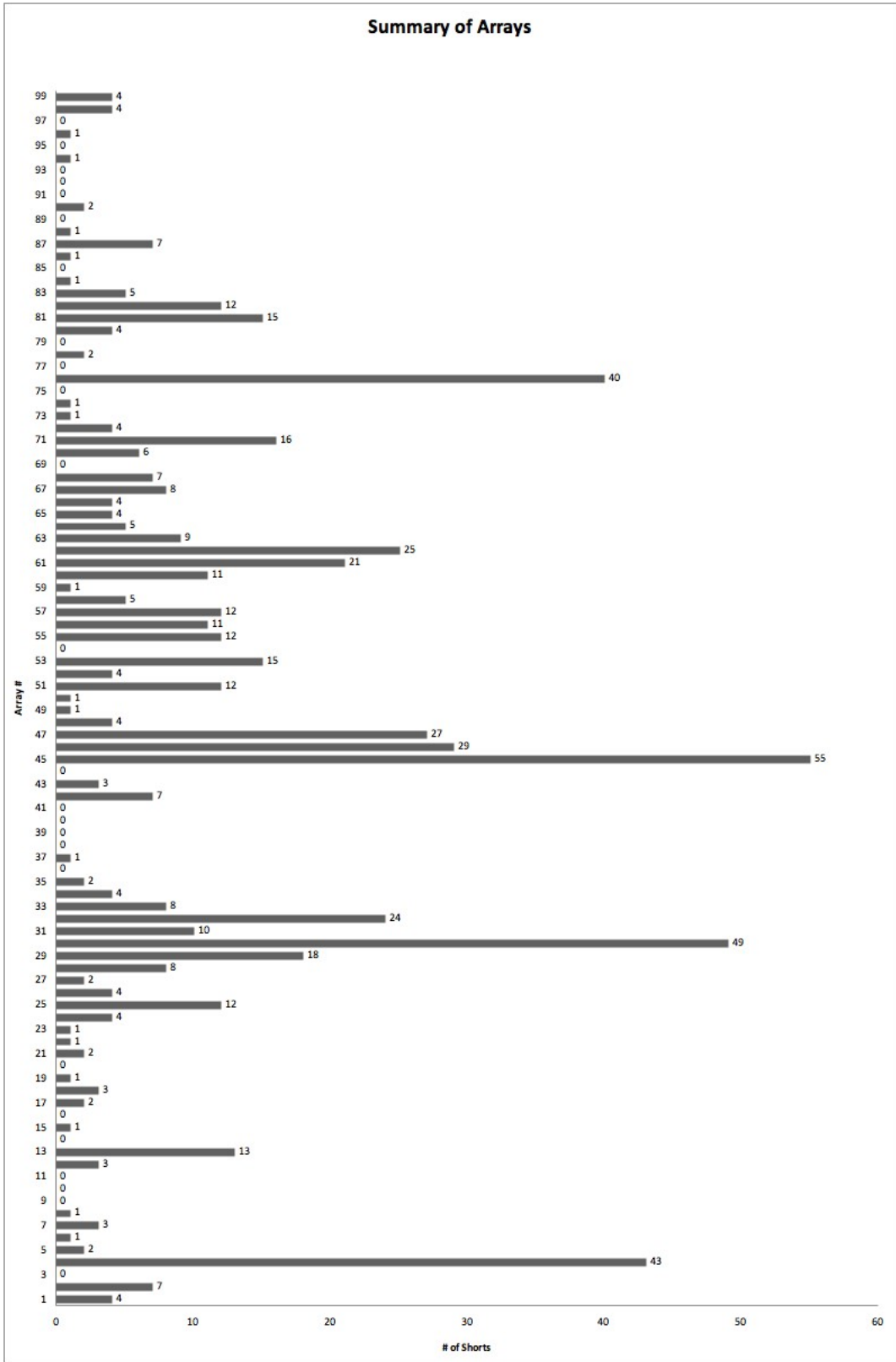
In addition, a histogram was made comparing all 60  $\mu\text{m}$  arrays to all 120  $\mu\text{m}$  arrays. Graph 7 shows the 60 micron arrays in red and the 120 micron arrays in blue. The vertical axis describes the percentage or fraction of arrays having a certain number of shorts, where all percentages must add to 100. The horizontal axis shows the number of shorts. The majority of all arrays, no matter what type, had somewhere between 0-15 shorts, but about 13% of both the 60 and 120 micron arrays had more than 14 shorts. In total, there were 18 arrays with the 120 micron spacing, and 81 arrays with 60 micron spacing. The number of 60 micron arrays with zero shorts is  $19 \pm 4.3$ , while the number of 120 micron arrays with zero shorts is  $6 \pm 2.4$ . However, the overall percentage of 60 micron arrays with zero shorts is  $\sim 23\%$  while that of the 120 micron arrays is 33%. The 120 micron arrays outperformed the 60 micron arrays because the fraction of them with zero shorts is one-

third larger than the fraction of 60 micron arrays with zero shorts. One discrepancy may arise due to the fabrication procedure of the arrays. Since the 60 micron arrays have smaller spacing between traces, there is a greater chance for dust particles or other pieces of metal to accidentally be attached between them. This leads to undesired connections between electrodes, causing a shorted impedance. The 120 micron arrays can avoid this problem since traces are spaced far enough apart that any pieces of metal remaining will not likely reach and form connections to an adjacent trace.



*Graph 7. Array histogram comparing 60 μm vs. 120 μm arrays.*

Next, Graph 6 and Table 3 show a summary of the number of shorts in all 99 arrays, listed in chronological order by array number. The table provides additional information regarding the exact locations of each shorted channel. For example, if the channel 12 was shorted, it refers to a shorted resistance that occurred between electrodes 12 and 13.



Graph 6. Summary of Arrays.

Array #	Array	# shorts	Channels Shorted
1	2--01--1	4	345-47, 360
2	2--01--2	7	175, 179, 198, 200-01, 399, 400
3	2--01--3	0	0
4	2--01--4	43	265-67, 347-81, 387, 390-91, 474-75
5	2--04--1	2	278, 382
6	2--04--2	1	506
7	2--04--3	3	457, 509, 510
8	2--04--4	1	99
9	2--07--1	0	0
10	2--07--2	0	0
11	2--07--3	0	0
12	2--07--4	3	3, 7, 8
13	2--09--1	13	175, 189, 404-05, 409-13, 417-19, 482
14	2--09--2	0	0
15	2--09--3	1	212
16	2--09--4	0	0
17	2--12--1	2	170, 249
18	2--12--2	3	131, 132, 254
19	2--12--3	1	93
20	2--12--4	0	0
21	2--13--1	2	149, 454
22	2--13--2	1	151
23	2--13--3	1	93
24	2--13--4	4	192-93, 290-91
25	2--15--1	12	27, 29, 265, 293, 302-03, 375, 394, 428, 436, 443-44
26	2--15--2	4	467-70
27	2--15--3	2	93, 319
28	2--15--4	8	166, 173-74, 321, 327, 345, 354, 356
29	1--1?--1	18	86-90, 213, 221, 230-31, 239-40, 285, 299, 388, 392, 402, 423, 426
30	1--1?--2	49	69-71, 113, 205-10, 220, 226, 229, 248, 250, 257-65, 321-23, 366, 381-83, 385-402
31	1--1?--3	10	71, 97, 104-06, 168, 247-48, 287, 301
32	1--1?--4	24	37, 74-82, 129-33, 388-94, 487-88
33	1--2?--1	8	12, 88-92, 142, 496
34	1--2?--2	4	130-33
35	1--2?--3	2	73, 123
36	1--2?--4	0	0
37	1--3?--1	1	309
38	1--3?--2	0	0
39	1--3?--3	0	0
40	1--3?--4	0	0
41	1--4?--1	0	0
42	1--4?--2	7	285-86, 375, 382-83, 409, 490
43	1--4?--3	3	366-68
44	1--4?--4	0	0
45	1--?#--1	55	3, 9, 10, 25-27, 36, 72, 86, 106, 117, 122, 134, 148, 151-54, 176-77, 179, 180, 211-13, 222, 234, 239, 240, 243-44, 246, 258, 262-63, 265, 267-68, 272, 280-81, 284, 286, 288, 319-20, 331, 339, 346, 352, 363, 394, 398, 489, 505
46	1--?#--2	29	19, 26, 73-75, 77, 96, 102, 105, 109, 113, 117-18, 122, 157, 165, 238, 242-43, 273-74, 291, 316, 343, 369-70, 379, 383, 435
47	1--?#--3	27	83, 84, 454-465, 467-479
48	1--?#--4	4	31, 390, 403, 462
49	1--03--1	1	491
50	1--03--2	1	324
51	1--03--4	12	215-19, 314-19, 425
52	2--02-1	4	48, 184, 293, 464
53	2--02-2	15	196, 293-300, 326, 334-37, 483

[3] Department of Psychological and Brain Sciences, Johns Hopkins University, "Systems Neuroscience, Exam Archive & Study Aids", [Online Resource], 2003 April, [cited 2009 Feb. 14], Available http:

<http://www.psy.jhu.edu/~fortune/Courses/systems/exams/exam-1/>

[4] Litke, A.M, et al., "What does the Eye Tell the Brain?: Development of a System for the Large-Scale Recording of Retinal Output Activity", IEEE Transactions on Nuclear Science, Vol. 51, No. 4, pgs 1434-1440, August 2004.

[5] Mastascusa, E.J., Professor of Electrical Engineering, Bucknell University, Lewisburg, Pennsylvania, "Unity Gain Buffer Amplifier", [Online Resource], 2008, [cited 2009 Feb. 14], Available http:

<http://www.facstaff.bucknell.edu/mastascu/eLessonsHTML/OpAmps/OpAmp2Note2Gain.html>

[6] Mathieson, K., et al., "Large-Area Microelectrode Arrays for Recording of Neural Signals", IEEE Transactions on Nuclear Science, Vol. 51, No. 5, pgs 2027-2031, October 2004.

[7] Norwegian University of Life Sciences, Oslo, Norway, "Computational Neuroscience", [Online Resource], 2008 December, [cited 2009 Feb. 11], Available http:

<http://arken.umb.no/~compneuro/extracellular.php>

[8] Opfer, J. E., Assistant Professor, Ohio State University, Honors Psychology, "Lecture: Neural Communication", [Online Resource], 2006, [cited 2009 Mar. 2], Available http: <http://faculty.psy.ohio-state.edu/opfer/H100/H00.PDFs/06-NeuralCom.pdf>

[9] Purves, D. Neuroscience 4<sup>th</sup> Ed., Sinauer Associates, Inc., 2008.